Journal of General Virology (2008), **89**, 2731–2740 DOI 10.1099/vir.0.2008/002212-0

Surface-expressed viral proteins in feline infectious peritonitis virus-infected monocytes are internalized through a clathrin- and caveolae-independent pathway

Hannah L. Dewerchin,[1] Els Cornelissen,[1] Evelien Van Hamme,[1] Kaatje Smits,[2]† Bruno Verhasselt[2] and Hans J. Nauwynck[1]

Correspondence
Hans J. Nauwynck
hans.nauwynck@UGent.be

[1]Laboratory of Virology, Faculty of Veterinary Medicine, Ghent University, Belgium

[2]Department of Clinical Chemistry, Microbiology and Immunology, Faculty of Medicine and Health Science, Ghent University, Belgium

Infection with feline infectious peritonitis virus (FIPV), a feline coronavirus, frequently leads to death in spite of a strong humoral immune response. In previous work, we reported that infected monocytes, the *in vivo* target cells of FIPV, express viral proteins in their plasma membranes. These proteins are quickly internalized upon binding of antibodies. As the cell surface is cleared from viral proteins, internalization might offer protection against antibody-dependent cell lysis. Here, the internalization and subsequent trafficking of the antigen–antibody complexes were characterized using biochemical, cell biological and genetic approaches. Internalization occurred through a clathrin- and caveolae-independent pathway that did not require dynamin, rafts, actin or rho-GTPases. These findings indicate that the viral antigen–antibody complexes were not internalized through any of the previously described pathways. Further characterization showed that this internalization process was independent from phosphatases and tyrosine kinases but did depend on serine/threonine kinases. After internalization, the viral antigen–antibody complexes passed through the early endosomes, where they resided only briefly, and accumulated in the late endosomes. Between 30 and 60 min after antibody addition, the complexes left the late endosomes but were not degraded in the lysosomes. This study reveals what is probably a new internalization pathway into primary monocytes, confirming once more the complexity of endocytic processes.

Received 18 March 2008
Accepted 29 June 2008

INTRODUCTION

Feline coronaviruses (FCoV) are spread worldwide and infect not only domestic cats but all members of the family *Felidae*. Infection with FCoV sometimes causes feline infectious peritonitis (FIP), a disease hallmarked by severe pleuritis/peritonitis and pyogranulomes. FCoV-infected cats often have high antibody titres. However, in FIP cats, these antibodies are not able to block infection even though the infected target cells (blood monocytes) do express viral proteins in their plasma membrane, allowing antibody-dependent complement-mediated cell lysis (Dewerchin *et al.*, 2005). Cell-mediated immunity is impaired in FIP cats, as lymphocytes and cytotoxic T cells are depleted (Haagmans *et al.*, 1996; Kipar *et al.*, 2001; Paltrinieri *et al.*, 2003). In previous work, we reported that the membrane-bound viral proteins, the spike and the membrane protein, are internalized upon antibody binding, which results in the loss of detectable viral proteins on the plasma membrane (Dewerchin *et al.*, 2006). The fact that no surface-expressed viral antigens can be found on FCoV-infected monocytes isolated from naturally infected FIP cats, and that surface expression returns after isolation and *in vitro* cultivation of the monocytes, is the first indication that this immune-evasion strategy also exists *in vivo* (Cornelissen *et al.*, 2007). If internalization could be blocked, then the humoral immune system would be able to contribute to the elimination of infected monocytes either by antibody-dependent complement-mediated or antibody-dependent cell-mediated lysis. This could open new perspectives for anti-feline infections peritonitis virus (FIPV) therapies. To elucidate how internalization can be blocked, the pathway needs to be identified.

Multiple pathways for ligand internalization have been described in literature and are represented in Fig. 1. There are four 'classical' pathways: phagocytosis, macropinocytosis, clathrin- and caveolae-mediated internalization. To

†Present address: Laboratoire de Vaccinologie et d'Immunologie Mucosale (LOVMI), Université Libre de Bruxelles, Belgium.

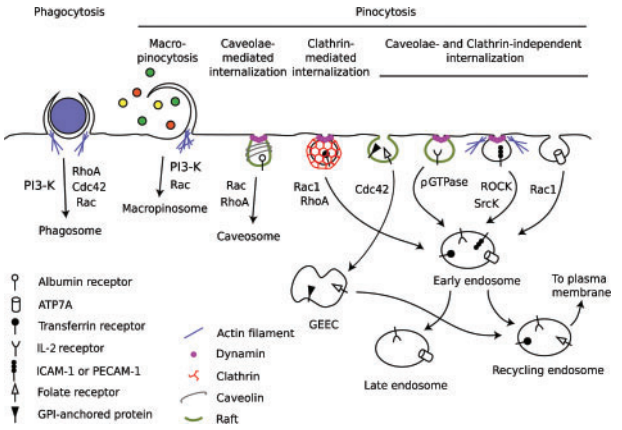

Fig. 1. Overview of all internalization pathways, showing characterizing features and subsequent intracellular trafficking. Phagocytosis is a process by which large pathogens, such as yeast or bacteria, are internalized by macrophages (Aderem & Underhill, 1999). Macropinocytosis is a mechanism for non-selective uptake of solute macromolecules that occurs upon cell stimulation (Swanson & Watts, 1995). In clathrin-mediated endocytosis, clathrin-coated invaginations form at the plasma membrane upon stimulation (Brodsky *et al.*, 2001). Caveolae are stationary flask-shaped invaginations that are present at the plasma membrane of many cell types, including monocytes/macrophages (Pelkmans & Helenius, 2002; Razani *et al.*, 2002). Four 'independent' internalization pathways have been described. The first one is the internalization pathway of interleukin-2 (IL-2) in leukocytes which is dynamin-, raft- and Rho-GTPase-dependent (Lamaze *et al.*, 2001). The second is the internalization pathway of the Menkes disease ATPase (a defective copper-transporting ATPase), which is Rac1- (a Rho-GTPase) dependent but raft- and dynamin-independent (Cobbold *et al.*, 2003). The third internalization pathway is that of GPI-anchored proteins, such as the folate receptor, which is raft- and Cdc42- (a Rho-GTPase) dependent but dynamin-independent (Sabharanjak *et al.*, 2002; Sabharanjak & Mayor, 2004). The fourth internalization pathway is used by intracellular adhesion molecule-1 (ICAM-1) and platelet–endothelial cell adhesion molecule-1 (PECAM-1); these are internalized after binding of anti-ICAM-1 or anti-PECAM-1 antibodies. This internalization pathway is dynamin-, actin-, Rho-kinase- and Src kinase-dependent but raft-independent (Muro *et al.*, 2003).

our knowledge, four clathrin- and caveolae-independent internalization or 'non-classical' pathways have been described.

This variety of internalization processes leads to several endocytic trafficking routes. After internalization, ligands are found in endosomes and will undergo sorting and further trafficking by mechanisms that are not completely understood. Some pathways will lead to the formation of specialized compartments, e.g. phagocytosis will bring ingested particles to the phagosome and later to the phagolysosome. Internalization through clathrin-coated pits can lead from the early endosomes to (i) the recycling endosomes and back to the plasma membrane, (ii) the late endosomes and then to the lysosome for degradation or (iii) delivery to the Golgi or the endoplasmic reticulum (ER) after passing through either the recycling or the late endosomes. These trafficking routes have also been described for clathrin- and caveolae-independent internalization pathways. Besides the different endocytic routes leading to different compartments, there is also some cross-talk between these compartments which allows exchange of ligands.

Here we used biochemical, cell biological and genetic approaches to determine the internalization method of surface-expressed FIPV antigens and their destination.

METHODS

Viruses and antibodies. A third passage of FIPV strain 79-1146 (ATCC) on feline cell line (CrFK) cells was used (McKeirnan *et al.*, 1981). Polyclonal anti-FCoV antibodies were kindly provided by P. Rottier (Utrecht University, The Netherlands). The antibodies were purified and biotinylated according to the manufacturer's instructions (Amersham Bioscience). Fluorescein isothiocyanate (FITC)-labelled polyclonal anti-FIPV antibodies were purchased from Veterinary Medical Research and Development (VMRD). The monoclonal antibody E22-2, recognizing the N-protein, was kindly provided by T. Hohdatsu (Kitasato University, Japan). The monocyte marker DH59B, recognizing CD172a, was purchased from VMRD. A rabbit polyclonal antibody against Rab 7 and goat polyclonal antibodies against early endosomal antigen 1 (EEA 1) and cathepsin D were purchased from Santa Cruz Biotechnology. Secondary antibodies and reagents [purchased from Molecular Probes (Invitrogen)] were goat anti-mouse–Texas red, goat anti-mouse–Alexa Fluor 350 (data not shown), streptavidin–Texas red, streptavidin–FITC and anti-rabbit– and anti-goat–Alexa Fluor 594 Zenon reagent.

Isolation and inoculation of blood monocytes. Four FCoV-, feline leukemia virus- and feline immunodeficiency virus-negative cats were used as blood donors. Blood (10 ml) was collected from the *vena jugularis* in heparin (15 U ml^{-1}) (Leo, Zaventem, Belgium) and mononuclear cells were separated on Ficoll-Paque (GE Healthcare). Cells were seeded on glass coverslips inserted into a 24-well dish, in RPMI 1640 medium containing 10 % fetal bovine serum (FBS), 0.3 mg glutamine ml^{-1}, 100 U penicillin ml^{-1}, 0.1 mg streptomycin ml^{-1}, 0.1 mg kanamycin ml^{-1}, 10 U heparin ml^{-1}, 1 mM sodium pyruvate and 1 % non-essential amino-acids (100 ×). Non-adherent cells were removed by washing the dishes twice with RPMI 1640, 2 and 24 h post-seeding (hps). The adherent cells consisted of 86 ± 7 % of monocytes (as assessed by fluorescent staining with the monocyte marker DH59B). Isolation efficiency fluctuated around 10 %. At 56 hps, monocytes were inoculated with FIPV at an m.o.i. of 5.

Internalization inhibition assays. Twelve hours after inoculation, monocytes seeded on glass coverslips were pre-incubated for 30 min at 37 °C with 5 % CO_2 with one of the following agents dissolved in RPMI (all from Sigma-Aldrich unless stated otherwise): 500 μM amantadine, 0.1 μM wortmannin, 0.74 nM *Clostridium difficile* toxin B, 20 μM latrunculin B (ICN Biochemicals), 10 mM methyl-β-cyclodextrin, 50 μg nystatin ml^{-1}, 40 μM dynamin inhibitory peptide (Tocris Cookson), 300 nM staurosporine, 10 mM sodium fluoride, 50 μg genistein ml^{-1} or 50 μM dephostatin (Calbiochem). The working concentration of each reagent was based on published values and was optimized qualitatively in internalization assays with control ligands (data not shown; see Supplementary Table S1, available in

JGV Online). Viability of the cells during the inhibition assay was tested for each inhibitor using ethidium bromide monoazide (Molecular Probes) and was always >99 %.

After pre-treatment, the cells were incubated with polyclonal biotinylated anti-FIPV antibodies in the presence of one of the given inhibitors for 30 min. Then, cells were fixed with 1 % formaldehyde, permeabilized with 0.1 % Triton X-100 and incubated with streptavidin–Texas red. Infected cells were visualized with polyclonal anti-FIPV–FITC. The glass coverslips were mounted on microscope slides using glycerin/PBS (0.9 : 0.1, v/v) with 2.5 % 1,4-diazabicyclo(2,2,2)octane and analysed using confocal microscopy. Monocytes were counted as cells with fully internalized antigen–antibody complexes when no labelling could be observed at the plasma membrane. Percentages of cells with fully internalized complexes were calculated relative to the total amount of monocytes that showed antibody binding, and thus had membrane expression before antibodies were added (about 50 % of the infected cells) (Dewerchin *et al.*, 2005). Because of the variability in the amount of cells with membrane expression, visualization of the complexes remaining at the plasma membrane was required. Therefore, an acid washing step to remove the extracellular antibodies was not performed.

To test the effectiveness of the reagents, a suitable control was used in each experiment. Monocytes seeded on glass coverslips were pre-incubated for 30 min with one of the inhibitors. After treatment, the cells were incubated with biotinylated human transferrin (Sigma-Aldrich) or fluorescent 1 μm polystyrene microspheres (FluoSpheres; Molecular Probes) in the presence of the inhibitor. Then, cells were fixed with formaldehyde and permeabilized with Triton X-100. The biotinylated transferrin was visualized with streptavidin–FITC; in cells incubated with fluorescent beads, actin was visualized with phalloidin–Texas red (Molecular Probes). The glass coverslips were mounted on microscope slides and analysed by confocal microscopy. For the controls, the monocytes were counted analogously to the FIPV-infected cells: ligands were considered 'fully internalized' when they were only observed inside the cell. Fluorescent beads were considered internalized when they were found inside the cortical actin labelling.

Transfer plasmid construction. The TRIPΔU3-CMV-WPRE vector [TRIPΔU3-CMV–GFP-WPRE in which green fluorescent protein (GFP) was deleted by *Bam*HI–*Sal*I digestion] was used as transfer vector, pMD.G was used as the envelope plasmid and p8.91 as the packaging plasmid as described by Stove *et al.* (2005).

Eps15 is a protein that is essential for the docking of adaptor protein-2 (AP-2) to the plasma membrane during the assembly of clathrin-coated pits (Benmerah *et al.*, 1998, 1999). The dominant-negative (DN) mutant of Eps15, named DIII, has a deletion at the Eps15 homology (EH) and coiled-coil domains and a C-terminal enhanced GFP (EGFP) tag. The construct D3Δ2, with an additional deletion of the AP-2-binding site, was used as a control. Both constructs were kindly provided by A. Benmerah and excised from pEGFP-C2 by *Bcl*I and *Eco*47III digestion and double-blunt cloned into TRIPΔU3-CMV-WPRE vector.

The EGFP-tagged wild-type (WT) and DN caveolin-1 constructs were a kind gift from A. Helenius (Kurzchalia *et al.*, 1992; Pelkmans *et al.*, 2001). The WT caveolin-1–GFP construct was amplified by PCR from the pEGFP-N1 vector and cloned into the TRIPΔU3-CMV-WPRE vector. The DN caveolin-1–GFP construct was excised from pEGFP-C1 by *Eco*47III and *Bam*HI digestion and double-blunt cloned into the TRIPΔU3-CMV-WPRE vector.

The EGFP-tagged WT and DN dynamin 2(aa) were kindly provided by M. McNiven (Cao *et al.*, 1998, 2000). Both constructs were excised from pEGFP-N1 by *Hin*dIII and *Xba*I digestion and double-blunt cloned into the TRIPDU3-CMV-WPRE vector.

Biological activity of all constructs was tested on CrFK cells before and after transfer to pTRIPΔU3-CMV-WPRE.

Production of lentiviral supernatant. 293FT cells (Invitrogen) were seeded in a 25 cm^2 culture dish in Iscove's modified Dulbecco's medium supplemented with 100 U penicillin ml^{-1}, 0.1 mg streptomycin ml^{-1} and 10 % heat-inactivated FBS. At 70 % confluency, cells were co-transfected with 1.66 μg packaging plasmids, 3.33 μg envelope plasmids and 3.33 μg transfer plasmids using a Calcium Phosphate Transfection kit (Invitrogen). Viral supernatant was harvested 40 h later.

Viral gene transfer, superinfection and internalization assays. Feline monocytes were isolated as described previously (Dewerchin *et al.*, 2005). After 3 h, the cells were washed and the medium was replaced with lentiviral supernatant. At 24 hps, cells were washed and fresh medium was added. At 56 hps, cells were inoculated with FIPV. Twelve hours later, internalization assays were performed by adding biotinylated anti-FIPV antibodies for 30 min. Then, cells were fixed with formaldehyde, permeabilized with Triton X-100 and incubated with streptavidin–Texas red to visualize the antigen–antibody complexes. Next, infected cells were visualized with anti-N monoclonal antibodies and goat anti-mouse–Alexa Fluor 350. Transduction efficiencies varied between 10 and 50 %.

For the controls, transduced cells were incubated with biotinylated transferrin or biotinylated cholera toxin B (Sigma-Aldrich). Then, cells were fixed and permeabilized, and ligands were visualized with streptavidin–Texas red.

Co-localization studies with endosomal markers. Twelve hours after inoculation, monocytes were incubated with biotinylated anti-FIPV polyclonal antibodies. At different times after antibody addition, cells were fixed and permeabilized, and antigen–antibody complexes were visualized with streptavidin–FITC followed by a blocking step with 10 % negative goat serum. To visualize early endosomes, goat polyclonal antibodies against EEA 1 were tagged with anti-goat–Alexa Fluor 594 Zenon reagent. To visualize late endosomes and lysosomes, rabbit polyclonal antibodies against Rab 7 and cathepsin D, respectively, were tagged with anti-rabbit–Alexa Fluor 594 Zenon reagent. After 45 min of incubation with the tagged antibodies, cells were fixed to stabilize the Zenon reagent. Finally, infected cells were visualized with anti-N monoclonal antibodies and goat anti-mouse–Alexa Fluor 350.

Confocal laser scanning microscopy. Samples were examined with a Leica TCS SP2 laser scanning spectral confocal system (Leica Microsystems) linked to a DM IRB inverted microscope (Leica Microsystems). Argon and helium–neon laser lights were used to excite FITC (488 nm line) and Texas red or Alexa Fluor 594 (543 nm line) fluorochromes. The images were obtained with Leica confocal software and processed with the GNU image manipulation program.

Statistical analysis. Triplicate assays were compared using a Mann–Whitney U test with SPSS 11.0. *P* values <0.05 were considered significantly different. For each assay, between 20 and 60 cells were counted.

RESULTS

Internalization of viral plasma membrane-bound proteins does not occur via phagocytosis or macropinocytosis

In vitro, around half of FIPV-infected monocytes display viral proteins on their plasma membrane (Dewerchin *et al.*,

2005). Binding of specific antibodies to these proteins leads to rapid internalization of the antigen–antibody complexes (Dewerchin *et al.*, 2006). In this paper we aimed to investigate the endocytic route through which the antigen–antibody complexes were internalized.

First, phagocytosis and macropinocytosis were tested as possible internalization routes using the inhibitors wortmannin and latrunculin B. Activity of the inhibitors was validated by determining their effect on the phagocytosis of fluorescent beads. Fig. 2(a) shows cells after the internalization assay in the presence of the inhibitors. The internalization of the control beads was reduced to 49 ± 11 and 18 ± 6 % of untreated controls for wortmannin and latrunculin B, respectively, while the antibody-induced internalization of viral proteins remained unaffected (Fig. 2b). These data suggest that viral proteins were not internalized via phagocytosis nor macropinocytosis and that internalization did not require dynamic actin.

Internalization of viral plasma membrane-bound proteins is not mediated by clathrin

Amantadine was used to test the dependence on clathrin. The internalization of viral antigens in the presence of amantadine was not significantly different from internalization in untreated monocytes, while internalization of the control ligand transferrin (a marker for clathrin-mediated endocytosis) was reduced to 2 ± 1 % of the internalization in untreated control cells (Fig. 2).

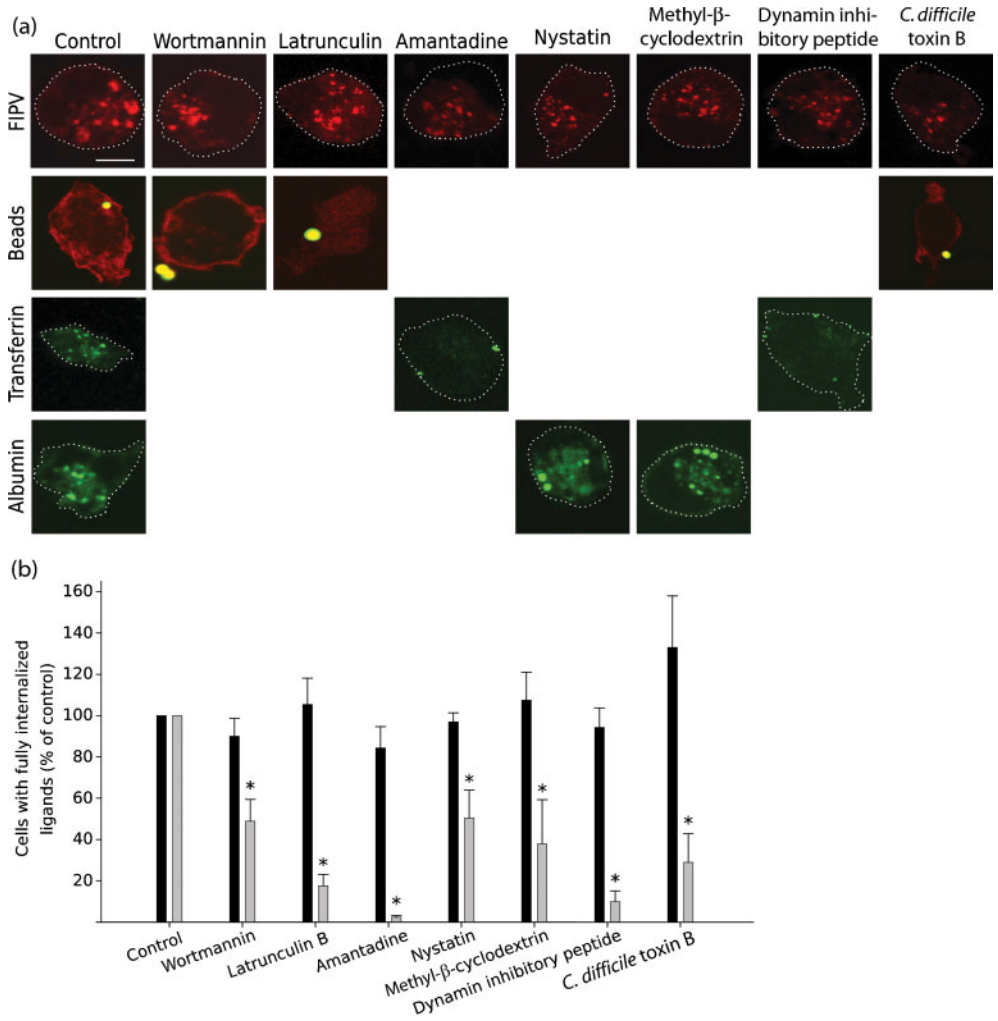

Fig. 2. Antibody-induced internalization of surface-expressed viral antigens in monocytes does not occur via a known internalization pathway. (a) Confocal images of feline monocytes after internalization assays in the presence of inhibitors. The images show a single optical section through the cell. In row 2, cortical actin was stained (red) to visualize whether the lamellipodia were closed around the beads. (b) Quantification of the internalization of viral antigens (solid bars) and control ligands (shaded bars) (beads, transferrin or albumin). Results are given relative to a control of untreated cells and show mean ± SD of triplicate assays. *, Results that are significantly different from the untreated control ($P<0.05$). Bar, 5 μm.

Possible independence of clathrin-mediated internalization was confirmed using a DN mutant of Eps15, named DIII. The construct D3Δ2 was used as a control. To enable expression of the DN protein in primary monocytes, the constructs were cloned into a lentiviral expression system. In monocytes transduced with DIII, the uptake of the control ligand transferrin was reduced to 40±9 %, while the internalization of viral proteins in DIII-transduced FIPV-infected monocytes remained unaffected (Fig. 3). The image of transferrin uptake in a monocyte transduced with DIII shows very little staining at the plasma membrane (Fig. 3). This is because internalization assays are performed when the DN proteins have been expressed for about 12 h. By that time, the transferrin receptors that are locked at the plasma membrane are mostly saturated by the unlabelled transferrin that is present in the culture medium. In monocytes transduced with the control construct D3Δ2, internalization of both transferrin and viral proteins was not significantly different from the untransduced controls. Together, these results indicate that antibody-induced internalization of viral antigens in FIPV-infected cells occurs independently of clathrin.

Internalization of viral plasma membrane-bound proteins is not mediated by caveolae

Nystatin was used to obtain the first indication of a possible role for caveolae in the internalization process. There was no significant influence of nystatin on the internalization of viral antigens, while the internalization of control ligand albumin, a marker for caveolae-mediated endocytosis, was reduced to 50±14 % of the untreated control (Fig. 2). Fig. 2(a) shows accumulation of albumin in the preformed caveolae that are locked underneath the plasma membrane, when monocytes are treated with nystatin or methyl-β-cyclodextrin. As illustrated in Fig. 2(a), the inhibitors were unable to completely block the internalization of caveolae in most monocytes.

The independence of the internalization process from caveolae was verified using a GFP-tagged DN mutant of caveolin-1, which was cloned into the lentiviral expression system (Kurzchalia *et al.*, 1992; Pelkmans *et al.*, 2001). GFP-tagged WT caveolin-1 was used as a control . In monocytes transduced with DN caveolin-1, there was no reduction in the internalization of viral antigens, whereas the uptake of the control ligand cholera toxin B was reduced to 40±5 % of the untransduced monocytes (Fig. 4). Transduction with WT caveolin did not have an effect on the internalization of viral proteins or cholera toxin B. Taken together, these results show that the internalization of viral surface-expressed proteins is not mediated by caveolae.

Internalization of viral plasma membrane-bound proteins does not occur via a known clathrin- and caveolae-independent pathway

Since the above results strongly suggest that internalization occurs through a clathrin- and caveolae-independent pathway, we wanted to compare the current pathway with the independent pathways described in the literature. In order to differentiate between the four independent pathways, three inhibitors were used: methyl-β-cyclodextrin, dynamin inhibitory peptide and *C. difficile* toxin B. None of the inhibitors caused a significant difference in the number of cells with fully internalized antigens. In contrast,

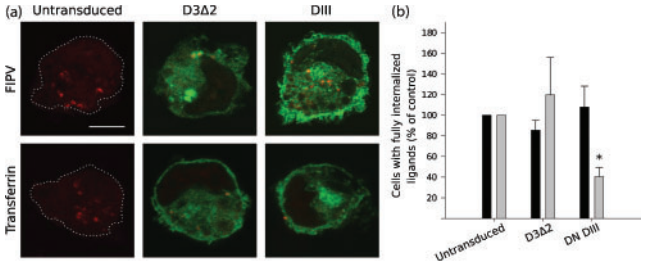

Fig. 3. Eps15 is not required during the internalization of viral membrane-bound proteins. Monocytes were transduced with DIII (DN Eps15) or the control construct D3Δ2. (a) Confocal images of feline monocytes after internalization assays. The images show a single optical section through the cell. The green signal represents the EGFP-tagged DIII or D3Δ2 proteins and the red signal represents biotinylated transferrin or antigen–antibody complexes visualized with streptavidin–Texas red. (b) Quantification of the internalization of viral antigens (solid bars) and the control ligand transferrin (shaded bars) relative to untransduced cells. Data represent the mean±SD of triplicate assays. *, Results that are significantly different from the untransduced control ($P<0.05$). Bar, 5 μm.

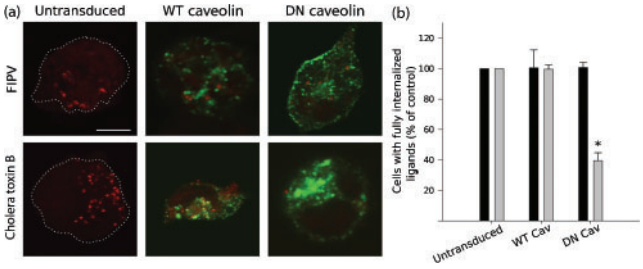

Fig. 4. Caveolin-1 is not required during the internalization of viral membrane-bound proteins. Monocytes were transduced with DN caveolin-1 or the control construct WT caveolin-1. (a) Confocal images of feline monocytes after internalization assays. The images show a single optical section through the cell. The green signal represents the EGFP-tagged WT or DN caveolin-1 proteins and the red signal represents biotinylated cholera toxin B or antigen–antibody complexes visualized with streptavidin–Texas red. (b) Quantification of the internalization of viral antigens (solid bars) and the control ligand cholera toxin B (shaded bars) relative to untransduced cells. Data represent the mean±SD of triplicate assays. *, Results that are significantly different from the untransduced control ($P<0.05$). Bar, 5 μm.

the internalization of the control ligands (albumin, transferrin or beads) was clearly inhibited to 38±21, 10±5 and 19±6 %, respectively, of the untreated controls (Fig. 2). Independence from rafts was also reinforced by the results with the inhibitor nystatin (Fig. 2).

To confirm the independence of dynamin, the only structural protein that characterizes two of the clathrin- and caveolae-independent pathways, a GFP-tagged DN mutant from dynamin (2aa) (K44A) was used (Cao *et al.*, 1998). GFP-tagged WT dynamin (2aa) was used as a control (Cao *et al.*, 2000). The constructs were cloned into the lentiviral expression system to allow expression in primary monocytes. Transduction of monocytes with the DN dynamin construct led to a decrease in uptake of the control ligand transferrin to 32±13 % of the untransduced control, while transduction with the WT dynamin construct lead to an increase to 161±21 %. In contrast, internalization of the viral antigen–antibody complexes remained unaffected by either construct (Fig. 5). These results indicate that dynamin, rafts and Rho-GTPases are not required for the internalization of viral antigens.

These findings also reinforce the independence from phagocytosis, since dynamin 2 is required for phagocytosis in macrophages, presumably at the stage of membrane extension (Gold *et al.*, 1999). Furthermore, the inhibitors methyl-β-cyclodextrin, dynamin inhibitory peptide and the DN dynamin construct confirmed these results, since they can block clathrin- and caveolae-mediated endocytosis (and two independent pathways) simultaneously.

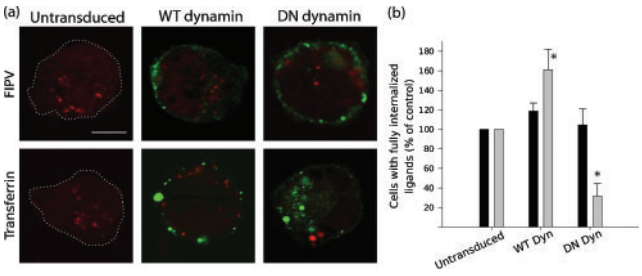

Fig. 5. Dynamin (2aa) is not required during the internalization of viral membrane-bound proteins. Monocytes were transduced with DN dynamin (2aa) or the control construct WT dynamin (2aa). (a) Confocal images of feline monocytes after internalization assays. The green signal represents the EGFP-tagged DN or DT dynamin (2aa) proteins and the red signal represents biotinylated transferrin or antigen–antibody complexes visualized with streptavidin–Texas red. (b) Quantification of the internalization of viral antigens (solid bars) and the control ligand transferrin (shaded bars) relative to untransduced cells. Data represent the mean ± SD of triplicate assays. *, Results that are significantly different from the untransduced control ($P<0.05$). Bar, 5 μm.

Internalization of viral antigens is regulated by a serine/threonine kinase

These data show that the proteins known to mediate internalization processes (actin, dynamin, clathrin and caveolin) were not required for internalization. To obtain an insight into the regulation of the internalization process presented here, the importance of phosphorylation and/or dephosphorylation was tested with chemical inhibitors. Representative confocal images of the internalization assays in the presence of inhibitors, and quantification of the results are given in Fig. 6.

Dephosphorylation. First, the importance of phosphatases for dephosphorylation was tested. Treatment with sodium fluoride, a broad range phosphatase inhibitor, did not reduce internalization, whereas internalization of the control ligand transferrin amounted to 46±6 % of the untreated control. In addition, treatment of cells with the more specific tyrosine phosphatase inhibitor, dephostatin, gave no reduction of internalized viral proteins (96±23 % of untreated control, in contrast to 2±3 % for the control ligand beads). These results indicated that phosphatases do not play a role in antibody-induced internalization.

Phosphorylation. Next, a role for kinases was investigated. Treatment with the broad range serine/threonine kinase inhibitor staurosporine resulted in a reduction in viral protein internalization (21±2 % of control) to a similar extent as the control ligand, beads (23±4 % of control). Fig. 6(a) shows an FIPV-infected monocyte without internalized viral proteins and a monocyte with partial internalization. Using the tyrosine kinase inhibitor genistein, the internalization of viral antigens amounted to 81±4 % of that of the untreated control, while the internalization of the control ligand albumin was 3±5 % of that of the untreated control. The reduction in internalization caused by genistein was significant but small compared with the control ligand albumin. This minor effect could be due to a non-specific action of the drug or it could be that tyrosine kinases play a role in the later stages of the internalization process, such as intracellular transportation. Taken together, these data indicate an important role for a serine/threonine kinase(s) in the antibody-induced internalization of surface-expressed viral proteins in FIPV-infected monocytes.

Co-localization of viral antigen–antibody complexes and endosomal compartments

After internalization, ligands are transported in endocytic compartments. To visualize this intracellular trafficking, co-localization stainings were performed with markers for early endosomes, late endosomes and lysosomes. First, passage through early endosomes was checked by staining EEA 1. The upper row of images in Fig. 7 shows that co-localization was only observed at 0.5 min. In most monocytes, few internalized antigen–antibody complexes

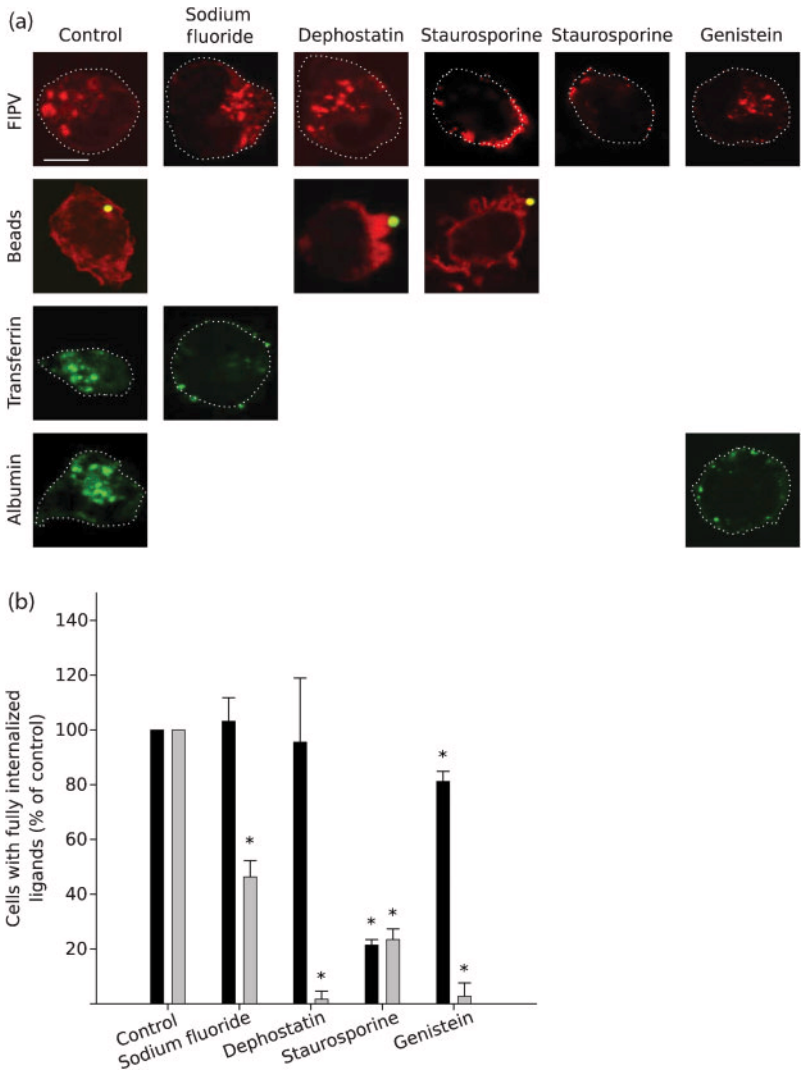

Fig. 6. Internalization of viral antigens is regulated by a serine/threonine kinase(s). (a) Confocal images of feline monocytes after the internalization assays performed in the presence of different inhibitors for serine/threonine or tyrosine phosphatases and serine/threonine or tyrosine kinases. In row 2, cortical actin was stained (red) to visualize whether the lamellipodia were closed around the beads. (b) Quantification of the internalization of viral antigens (solid bars) and the control ligand (shaded bars) (beads, transferrin or albumin). Results are given relative to a control of untreated cells and indicate mean ± SD of triplicate assays. *, Results that are significantly different from the untreated control ($P<0.05$). Bar, 5 μm.

were found to co-localize with EEA 1. This indicates that the antigen–antibody complexes resided in early endosomes only briefly before they were transported further into the cell. Co-localization staining with Rab 7 (a late endosome marker) confirmed that the antigen–antibody complexes moved quickly to the late endosomes, in which complexes were observed as soon as 1 min after internalization (Fig. 7, middle row). The antigen–antibody complexes accumulated in the late endosomes until 30 min after antibody addition. By 60 min, all complexes had left the late endosomes. Staining with the lysosome marker cathepsin D showed no co-localization at any time point (Fig. 7, lower row).

DISCUSSION

Internalization processes have been studied for decades; phagocytosis was the first endocytic process to be described over 100 years ago (Metchnikoff, 1905). In 1931, membrane ruffles were seen on macrophages, a phenomenon that was later named macropinocytosis (Lewis, 1931). In the 1950s, electron microscopists described cave-like invaginations at the plasma membrane, which were called ‘caveolae intracellulare’. However, it took until 1992 for the major structural protein, caveolin, to be identified (Rothberg *et al.*, 1992). In 1964, internalization through vesicles covered with a dense protein coat was first described (Roth & Porter, 1964). It took another 10 years for the major coat protein, clathrin, to be characterized (Pearse, 1975). Since then, knowledge about these four ‘classical’ internalization pathways has been gathered at increasing speed. Around the turn of the century, the first clathrin- and caveolae-independent pathways were reported (Gilbert & Benjamin, 2000; Lamaze *et al.*, 2001). To date, four independent pathways have been described, two of which involve dynamin for pinching off the vesicle from the plasma membrane. For the other two, no structural protein has been identified so far. They are distinguished from each other solely by the finding that they are mediated by different Rho-GTPases. There are several reports of viruses using an independent pathway for

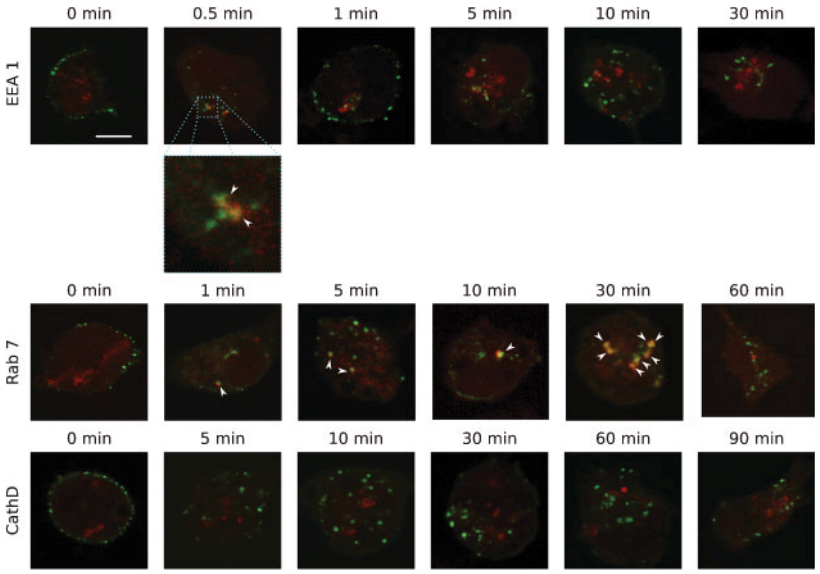

Fig. 7. After passage through the early endosomes, viral antigens accumulate in the late endosomes but are not degraded in the lysosomes. Internalizing antigen–antibody complexes were visualized with streptavidin FITC (green signal). EEA 1, Rab 7 and cathepsin D were used as markers for early endosomes, late endosomes and lysosomes, respectively (red signal). The images show a single optical section through a monocyte. Bar, 5 μm.

entry into the host cell, although most pathways have not been characterized fully (Gilbert & Benjamin, 2000; Gilbert *et al.*, 2003; Sanchez-San Martin *et al.*, 2004; Damm *et al.*, 2005; Van Hamme *et al.*, 2008).

In this work, we sought to identify the pathway through which the surface-expressed viral proteins in FIPV-infected monocytes were internalized after binding of antibodies. The techniques that were used were based on immunofluorescence and confocal microscopy. Considering the fact that the *in vitro* infection rate of monocytes varies between 0.1 and 1 %, of which around 50 % have membrane expression, experiments that require a lot of starting material (e.g. flowcytometry or Western blots) could not be performed. In addition, we were restricted to monocytes to perform our experiments since internalization cannot be induced in CrFK or fcwf cell lines (Dewerchin *et al.*, 2006).

The surface-expressed viral proteins in a FIPV-infected monocyte are the spike protein and the membrane protein (Dewerchin *et al.*, 2006). The experiments presented here showed that internalization of these proteins was not clathrin-mediated, since it could not be blocked by any of the six inhibitors (amantadine, latrunculin B, methyl-β-cyclodextrin, dynamin inhibitory peptide, *C. difficile* toxin B and sodium fluoride) or two DN constructs (eps15 and dynamin) that are known to inhibit clathrin-mediated internalization. Independence from caveolae was also confirmed by using the six inhibitors and two DN constructs. The experiments further indicated that the antigen–antibody complexes were internalized via a new pathway regulated by a serine/threonine kinase(s) but not by phosphatases or tyrosine kinases. Future research will focus on identifying which serine/threonine kinase(s) is of importance.

After internalization, the viral antigen–antibody complexes were further transported into the cell. The main pinocytic trafficking routes are the recycling and the degradative pathway (Mellman, 1996). In the internalization process studied here, internalized antigen–antibody complexes could be observed inside the cell for more than 1 h, making the recycling pathway a highly unlikely route for trafficking. Therefore, co-localization stainings with markers for the degradative endocytic pathway were performed. The stainings revealed that the antigen–antibody complexes resided in the early endosomes only briefly, followed by accumulation of the antigen–antibody complexes in the late endosomes. The complexes left the late endosome between 30 and 60 min but were not observed in the lysosomes, indicating that they did not follow the degradative pathway. The fact that the antigen–antibody complexes could still be observed 90 min after antibody addition confirmed that the complexes were not degraded. It remains to be elucidated whether these antigen–antibody complexes might be of importance during the infection cycle. A model for the internalization pathway combining all the results is given in Fig. 8.

The finding that internalization of the viral antigen–antibody complexes occurs through an unusual pathway actually increases the chance that blocking of internalization could be used as a treatment for FIP cats. We have shown previously that internalization could not be reproduced in the feline CrFK and fcwf cell lines (Dewerchin *et al.*, 2006). This implies that specific cellular components are required that are not ubiquitously expressed, adding to the likelihood of finding a compound that will specifically block this internalization route while leaving the more conventional pathways undisturbed.

In previous reports, we described three patterns of FIPV infection kinetics in monocytes: (i) sustained infection, (ii) no sustained infection and (iii) no infection (Dewerchin *et al.*, 2005). For the experiments in the current paper, monocytes from cats belonging to the first and second

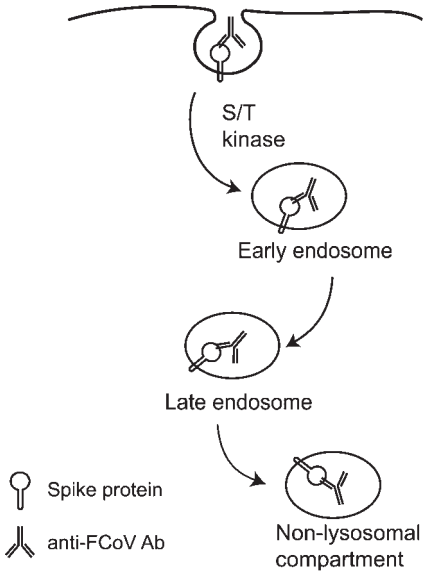

Fig. 8. Model for the internalization of surface-expressed viral proteins in FCoV-infected monocytes.

pattern were used (at 12 h post-inoculation). No differences were observed in the amount of cells with membrane expression or in the percentage of cells that showed internalization both in the presence or absence of inhibitors. This indicates that internalization is not cat-dependent and that all FCoV-infected monocytes internalize their viral proteins via the same pathway. Even though only about 1 % of the monocytes was infected with FIPV, the fact that every infected monocyte was able to internalize its viral proteins adds to the likelihood that internalization occurs *in vivo* as well. In addition, we have found that FCoV-infected monocytes in naturally infected FIP cats show no membrane expression (Cornelissen *et al.*, 2007). However, membrane expression returns after *in vitro* cultivation, which indicates that internalization might occur *in vivo*. By further characterizing this internalization pathway *in vitro* and determining which cellular proteins are of importance, we will be able to verify whether viral proteins in naturally infected monocytes are internalized via the same pathway.

In conclusion, surface-expressed viral proteins in FIPV-infected monocytes are internalized through a clathrin- and caveolae-independent internalization pathway that is independent of actin, rafts, dynamin, Rho-GTPases, phosphatases and tyrosine kinases, but dependent on a serine/threonine kinase(s). Internalization of viral antigens through this pathway led to trafficking via the early endosomes to the late endosomes but not to the lysosomes. Despite the growing number of independent internalization pathways, very little is known about the molecular mechanisms underlying these pathways. But, as the pathways are better characterized, it is becoming apparent that they are very well regulated by the cell itself and by the ligand that is being internalized. Undoubtedly, more internalization pathways await discovery and characterization, which might lead to a better understanding of the complex network of all internalization processes.

ACKNOWLEDGEMENTS

H. L. D. and E. C. were supported by the Institute for the Promotion of Innovation through Science and Technology in Flanders (IWT-Vlaanderen). E. V. H. was supported by the Special Research Fund of Ghent University, grant 01D29005. K. S. is a PhD fellow and B. V. a senior clinical investigator supported by the Research Foundation Flanders (FWO), grant G.0061.05. We are very grateful to P. Rottier for supplying polyclonal anti-FCoV antibodies and to T. Hohdatsu for monoclonal anti-N-protein antibodies; to A. Benmerah for the DIII and D3Δ2 constructs, to A. Helenius for the WT and DN caveolin-1 constructs, to M. McNiven for the WT and DN dynamin 2 constructs and to J. Vicca for supplying fluorescent beads. We thank E. Naessens for technical assistance and J. Vandekerckhove and C. Ampe for critical reading.

REFERENCES

Aderem, A. & Underhill, D. (1999). Mechanisms of phagocytosis in macrophages. *Annu Rev Immunol* **17**, 593–623.

Benmerah, A., Lamaze, C., Begue, B., Schmid, S., Dautry-Varsat, A. & Cerf-Bensussan, N. (1998). AP-2/Eps15 interaction is required for receptor-mediated endocytosis. *J Cell Biol* **140**, 1055–1062.

Benmerah, A., Bayrou, M., Cerf-Bensussan, N. & Dautry-Varsat, A. (1999). Inhibition of clathrin-coated pit assembly by an Eps15 mutant. *J Cell Sci* **112**, 1303–1311.

Brodsky, F. M., Chen, C.-Y., Knuehl, C., Towler, M. C. & Wakeham, D. E. (2001). Biological basket weaving: formation and function of clathrin-coated vesicles. *Annu Rev Cell Dev Biol* **17**, 517–568.

Cao, H., Garcia, F. & McNiven, M. (1998). Differential distribution of dynamin isoforms in mammalian cells. *Mol Biol Cell* **9**, 2595–2609.

Cao, H., Thompson, H., Krueger, E. & McNiven, M. (2000). Disruption of golgi structure and function in mammalian cells expressing a mutant dynamin. *J Cell Sci* **113**, 1993–2002.

Cobbold, C., Coventry, J., Ponnambalam, S. & Monaco, A. (2003). The menkes disease ATPase (ATP7A) is internalized via a Rac1-regulated, clathrin- and caveolae-independent pathway. *Hum Mol Genet* **12**, 1523–1533.

Cornelissen, E., Dewerchin, H., Van Hamme, E. & Nauwynck, H. (2007). Absence of surface expression of feline infectious peritonitis virus (FIPV) antigens on infected cells isolated from cats with FIP. *Vet Microbiol* **121**, 131–137.

Damm, E.-M., Pelkmans, L., Kartenbeck, J., Mezzacasa, A., Kurzchalia, T. & Helenius, A. (2005). Clathrin- and caveolin-1-independent endocytosis: entry of simian virus 40 into cells devoid of caveolae. *J Cell Biol* **168**, 477–488.

Dewerchin, H. L., Cornelissen, E. & Nauwynck, H. J. (2005). Replication of feline coronaviruses in peripheral blood monocytes. *Arch Virol* **150**, 2483–2500.

Dewerchin, H. L., Cornelissen, E. & Nauwynck, H. J. (2006). Feline infectious peritonitis virus-infected monocytes internalize viral membrane-bound proteins upon antibody addition. *J Gen Virol* **87**, 1685–1690.

Gilbert, J. M. & Benjamin, T. L. (2000). Early steps of polyomavirus entry into cells. *J Virol* **74**, 8582–8588.

Gilbert, J. M., Goldberg, I. & Benjamin, T. L. (2003). Cell penetration and trafficking of polyomavirus. *J Virol* **77**, 2615–2622.

Gold, E. S., Underhill, D. M., Morrissette, N. S., Guo, J., McNiven, M. A. & Aderem, A. (1999). Dynamin 2 is required for phagocytosis in macrophages. *J Exp Med* **190**, 1849–1856.

Haagmans, B. L., Egberink, H. F. & Horzinek, M. C. (1996). Apoptosis and T-cell depletion during feline infectious peritonitis. *J Virol* **70**, 8977–8983.

Kipar, A., Kohler, K., Leukert, W. & Reinacher, M. (2001). A comparison of lymphatic tissues from cats with spontaneous feline infectious peritonitis (FIP), cats with FIP virus infection but no FIP, and cats with no infection. *J Comp Pathol* **125**, 182–191.

Kurzchalia, T. V., Dupree, P., Parton, R. G., Kellner, R., Virta, H., Lehnert, M. & Simons, K. (1992). VIP21, a 21kD membrane protein is an integral component of trans-golgi-derived transport vesicles. *J Cell Biol* **118**, 1003–1014.

Lamaze, C., Dujeancourt, A., Baba, T., Lo, C., Benmerah, A. & Dautry-Varsat, A. (2001). Interleukin 2 receptors and detergent-resistant membrane domains define a clathrin-independent endocytic pathway. *Mol Cell* **7**, 661–671.

Lewis, W. H. (1931). Pinocytosis. *Johns Hopkins Hosp Bull* **49**, 17–27.

McKeirnan, A. J., Evermann, J. F., Hargis, A., Miller, L. M. & Ott, R. L. (1981). Isolation of feline coronaviruses from two cats with diverse disease manifestations. *Feline Pract* **11**, 16–20.

Mellman, I. (1996). Endocytosis and molecular sorting. *Annu Rev Cell Dev Biol* **12**, 575–625.

Metchnikoff, E. (1905). *Immunity in Infective Diseases.* Cambridge: Cambridge University Press.

Muro, S., Wiewrodt, R., Thomas, A., Koniaris, L., Albelda, S., Muzykantov, V. & Koval, M. (2003). A novel endocytic pathway induced by clustering endothelial ICAM-1 or PECAM-1. *J Cell Sci* **116**, 1599–1609.

Paltrinieri, S., Ponti, W., Comazzi, S., Giordano, A. & Poli, G. (2003). Shifts in circulating lymphocyte subsets in cats with feline infectious peritonitis (FIP): pathogenic role and diagnostic relevance. *Vet Immunol Immunopathol* **96**, 141–148.

Pearse, B. M. (1975). Coated vesicles from pig brain: purification and biochemical characterization. *J Mol Biol* **97**, 93–98.

Pelkmans, L. & Helenius, A. (2002). Endocytosis via caveolae. *Traffic* **3**, 311–320.

Pelkmans, L., Kartenbeck, J. & Helenius, A. (2001). Caveolar endocytosis of simian virus 40 reveals a new two-step vesicular-transport pathway to the ER. *Nat Cell Biol* **3**, 473–483.

Razani, B., Woodman, S. & Lisanti, M. (2002). Caveolae: from cell biology to animal physiology. *Pharmacol Rev* **54**, 431–467.

Roth, T. F. & Porter, K. R. (1964). Yolk protein uptake in the oocyte of the mosquito *Aedes aegypti*. *J Cell Biol* **20**, 313–332.

Rothberg, K. G., Heuser, J. E., Donzell, W. C., Ying, Y. S., Glenney, J. R. & Anderson, R. G. (1992). Caveolin, a protein component of caveolae membrane coats. *Cell* **68**, 673–682.

Sabharanjak, S. & Mayor, S. (2004). Folate receptor endocytosis and trafficking. *Adv Drug Deliv Rev* **56**, 1099–1109.

Sabharanjak, S., Sharma, P., Parton, R. & Mayor, S. (2002). GPI-anchored proteins are delivered to recycling endosomes via a distinct Cdc42-regulated, clathrin-independent pinocytic pathway. *Dev Cell* **2**, 411–423.

Sanchez-San Martin, C., Lopez, T., Arias, C. & Lopez, S. (2004). Characterization of rotavirus cell entry. *J Virol* **78**, 2310–2318.

Stove, V., Van de Walle, I., Naessens, E., Coene, E., Stove, C., Plum, J. & Verhasselt, B. (2005). Human immunodeficiency virus Nef induces rapid internalization of T-cell coreceptor CD8α-β. *J Virol* **79**, 11422–11433.

Swanson, J. A. & Watts, C. (1995). Macropinocytosis. *Trends Cell Biol* **5**, 424–428.

Van Hamme, E., Dewerchin, H. L., Cornelissen, E., Verhasselt, B. & Nauwynck, H. J. (2008). Clathrin- and caveolae-independent entry of feline infectious peritonitis virus in monocytes depends on dynamin. *J Gen Virol* **89**, 2147–2156.